

High resolution images obtained with uncooled microbolometer

J. Sadi ¹, A. Crastes ²

¹ LIGHTNICS – 177b avenue Louis Lumière – 34400 Lunel - France

² ULIS SAS, ZI Veurey Voroize - BP27 - 38113 Veurey Voroize, France

Abstract

This study presents experimental results of a resolution enhancement algorithm used in the physical world without any microscan optomechanical element. The HR (High Resolution) software developed by Lightnics was used together with an uncooled microbolometer array from Ulis, with low thermal time constant. It takes advantage of the relative motion between camera and object to produce information redundancy through a set of captured images giving rise to one increased resolution image. Enhanced images from a bar target show better MTF and MRTD curves after HR software processing than before. In addition, lower spatial and temporal noises were obtained as an additional benefit of the algorithm.

Keywords: aliasing, under sampled, high resolution, super resolution, infrared sensor, uncooled microbolometers.

INTRODUCTION

A major drawback in infrared sensors has long been a lack of resolution. An increase in image resolution is often sought to enable visualization of details in the image, in order to get a proper identification of objects in the vision field. Such details are lost particularly when using low f# in the imaging system. In this case the spot size is well beneath the pixel size of the imaging system. Consequently, the resultant pixel intensity is a mean between a number of image spots, so we lose information on each individual spot.

Such a situation arises in the infrared domain as low f# are preferably used. However, this limitation can be overcome by proper deinterlacing of those image spots through the use of a specific algorithm. Thanks to the increase in computing power of DSP (Digital Signal Processors), such an algorithm can now be implemented in electronics boards for real time processing at video rate. But as this algorithm needs a number of input standard resolution images to compute a single output high resolution frame, it requires an image sensor with low thermal time constant. As a consequence, uncooled microbolometers are the “preferred” option for resolution enhancement in the infrared domain.

However, one key point to bear in mind before performing the electronics implementation of such an algorithm is to assess the effectiveness of the computed temporal interpolation. Here we will particularly emphasize this central point by providing results of our analysis of the high resolution images obtained compared with the low resolution ones. To this end, we will discuss the influence of the algorithm on a) the MTF (Modulation Transfer Function), b) both the temporal and spatial NETD (Noise Equivalent Temperature Difference), and c) the MRTD (Minimum Resolvable Temperature Difference) of the infrared imaging system.

1. HIGH RESOLUTION ENHANCEMENT

Let a set $\{n_i\}$ of low resolution images be captured by an infrared imaging system based on an uncooled microbolometer array. In order to deinterlace individual spots mixed together in each image of this set and to extract the detailed information, we must first reference all the images of this set according to the first one. Doing so, we will have a perfect location correspondence of the same object between any two images in this set. This will ensure that every object in the observed scene will be positioned at the same location in each image. This process is done by applying a translation operator to each image in the case of global motion of the scene. The vector parameter of this translation operator may, e.g., be calculated by a phase correlation technique [1]:

$$C = \frac{I_0 I_j^*}{I_0 I_j^*}$$

where I_0 is the reference image and I_j is a given image in the set $\{n_i\}$.

In order for this correlation to be more effective, it is advisable to perform some preprocessing operations on the input set of low resolution images. Such preprocessing operations depend on the particular difficulties involved by the observed scene. Low contrast scenes, for example, may benefit from histogram equalization in the preprocessing scheme.

Once every image I_j of the set has been translated according to the common reference given by the first image I_0 , it is possible to enter the reconstruction process.

The second step, *i.e.* the reconstruction process, is made difficult by many factors affecting image quality: varying lighting, and in general: scene- conditions, lost information in the background noise and digital conversion with limited number of digits. The limited dynamic and the electronic noise both put a limit on, respectively, the perceivable contrast and detail size. Consequently, they both degrade the MTF of the imaging system. High resolution reconstruction is meant to improve this degraded MTF by acting on the contrast and the detail size. The former is enhanced through a decrease of the noise, which gives rise to a better signal to noise ratio, while the latter is decreased by proper reorganization of individual low resolution pixels into a larger image matrix.

High resolution reconstruction is known to be an “ill-posed inverse problem”, that is: a problem which cannot be solved by classical inversion methods, such as linear inversion. In other words, one set of low resolution images could give rise to a number of resulting high resolution solutions. It is then often difficult to reach the exact solution without adding a priori constraints regarding the nature of the scene. This is why neural networks [2], approximate matrix inversion methods [3], statistics based on Markov random fields [4] or convex sets, may be used. However these are time consuming methods since for real time implementation it is often desirable to speed up the calculation process. In addition, the presence of noise on infrared images requires to use some type of regularization process such as Tikhonov regularization [5] for example.

Our method involves additional constraints to perform this regularization in the form of a known set of LR (Low Resolution) images and a known optical transfer process. Let the imaging process be modeled through the following equation:

$$Y_{obs} = K.X + N$$

where Y_{obs} are the observed LR images, X represents the true scene to be perceived, K is a kernel that accounts for the degradation process (via blurring, motion and subsampling) and N stands for the noise. Our aim is to reach X based on the knowledge of a set of slightly different occurrences of Y_{obs} .

In order to constrain the solution space such an iterative method usually proceeds by comparing a set of estimated low resolution images Y_{sim} with the set of captured real images Y_{obs} . We then look for the minimum of a least square criterium:

$$\|Y_{obs} - K.Y_{sim}\|^2 + a\|HPF(Y_{sim})\|^2,$$

where a is the regularization parameter and HPF means High Pass Filter. Our method thus rests on a careful parametrization of this stop condition, which then leads to a fairly good approximation of the exact solution.

The estimated images are computed through precise modeling of the imaging system. This step thus requires to properly calibrate the camera beforehand, to reach such system parameters as its point spread function (PSF) and the transfer function of the pixels used in the microbolometer array. This modeling gives rise to the convolution kernel K that can be used in the further degradation process.

The HR image is then improved after each iteration by using a convergence parameter b according to:

$$Y_{sim}^{i+1} = Y_{sim}^i + b\left[K'(Y_{obs} - K.Y_{sim}^i) - aA(Y_{sim}^i)\right],$$

where K' is an upsampling and warping function, and A is a regularization operator.

The block-diagram of our algorithm logic is thus as follows:

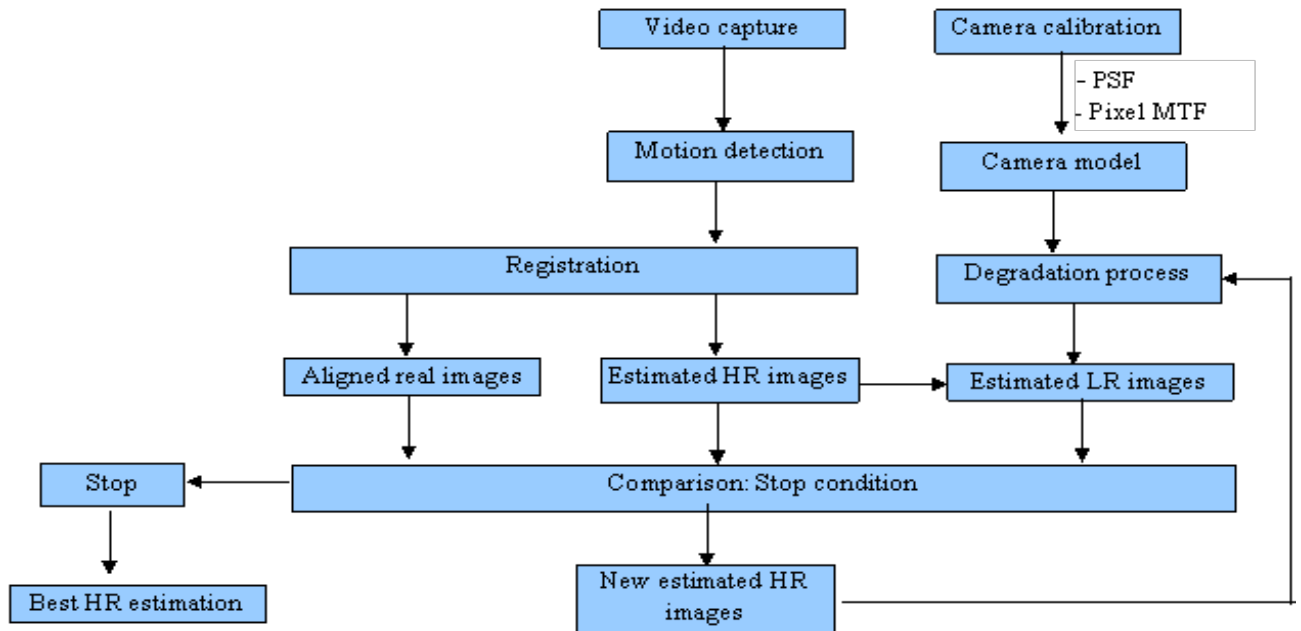


Figure 1: High-resolution processing block-diagram

In order to put this HR algorithm to the test, we have compared the image quality of standard resolution images (« real images » in the block-diagram above) and of increased resolution images (« Best HR estimation » in the block-diagram above).

2. ALGORITHM EVALUATION

2.1 Procedure

In the following, our purpose was to assess the performance of the algorithm through evaluation in real conditions, that is: with physical target and camera as opposed to simulated scene and camera.

In order to evaluate the above mentioned Lightnics algorithm, we used a thermoelectric bar target with 4 bars of width $\frac{1}{2}$ inch each, spaced by $\frac{1}{2}$ inch, together with a microbolometer array comprising 160 x 120 pixels with a pitch of 25 μ m (UL 02 15 2).

We captured 11 films at various distances from the target, ranging from 2 to 15 meters. The corresponding spatial frequencies thus range from 4.4 lp/mm to 32.8 lp/mm.

Each film was 150 images long and each pixel image was coded by 16 bits.

A Janos objective (Tyto Series) was used in front of the sensor with a 18 mm focal length and f# of 1.

After the 11 films were captured, several profiles across the bar target were selected in various images of each film. These profiles enabled us to compute the mean contrast for each film. By plotting these contrasts versus spatial frequency, we obtained the contrast transfer function (CTF) of the imaging system.

Interpolation of the CTF is then necessary to gain access to CTF at precise distances needed to convert CTF data to the modulation transfer function (MTF). We thus applied to the CTF a fitting with a polynomial expansion of sixth degree before using Coltman formula to convert to the MTF [6].

In order to gain access to the MRTD, we also had to evaluate the rms noise from the video captured. The fixed pattern spatial noise was determined by averaging the image sequence to obtain a single averaged image from which the spatial noise standard deviation was derived.

Temporal rms noise was obtained by computing the standard deviation of all pixels located at a given position in the entire set of the image sequence.

Instead of changing the 4 bar-target frequency to have access to different spatial frequency, we adjust the distance between the 4 bar target and the sensor, the optics being focused at the infinite.

Then, the spatial frequency according to the distance is given by: $\nu(\text{cycles} / \text{mm}) = \frac{10^{-3} \cdot d}{f \cdot \lambda}$,

where d is the distance (in meters) between the 4 bar-target and the sensor, λ is the cycle length at the target and is f the optical effective focal length chosen short to be able to make the measurement into our lab (distance limited).

An important and fundamental point is to be sure that the spatial resolution limitation is due to the detector itself and not to the optics. That is why we have worked on the optical axis (center of the image). The gain bringing by this method will be greater (or at least more visible) in the case where the detector is clearly the limiting factor in term of spatial resolution (large pixel pitch compared to the optical diffraction limited or low fill factor).

The interest to choose a short EFL for the optics was to obtain the Nyquist frequency for a distance compatible with our lab surface.

2.2 Results

The contrasts measured for each film taken at a given distance have been processed with bilinear interpolation to enable contrast evaluation at the zero spatial frequency. By normalizing contrasts values with respect to the value at the zero spatial frequency, we compute the CTF appearing in figure 2.

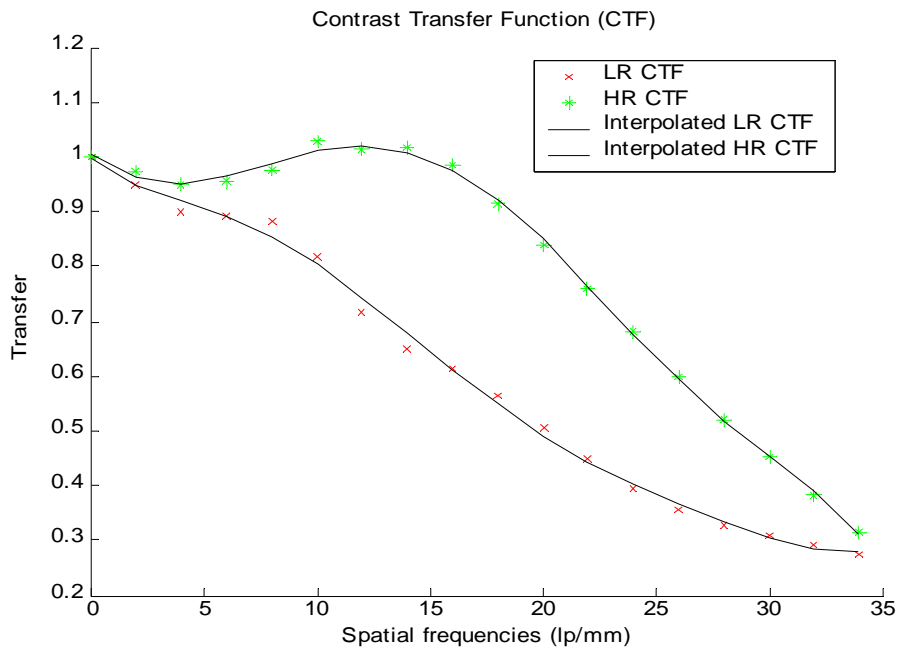


Figure 2: CTF computed with low resolution (LR) images and high resolution (HR) enhanced images.

These CTF gives rise, using Coltman relationship, to the MTF for both conditions: images with and without high resolution enhancement, as can be seen on figure 3.

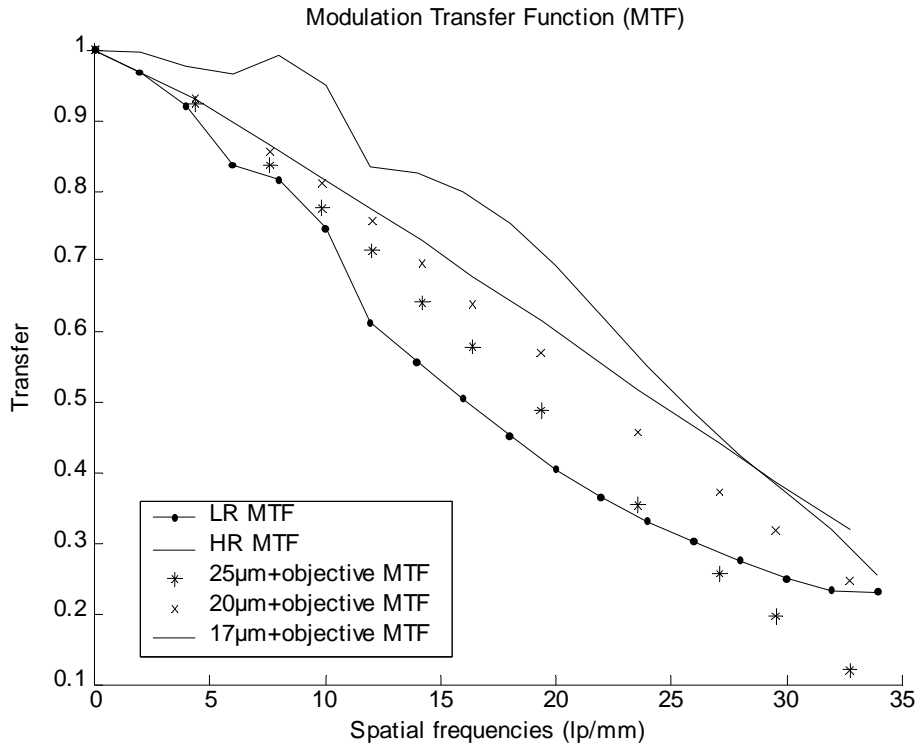


Figure 3: MTF for films with and without HR processing compared to various imaging system MTFs. We notice the good agreement between experimental data and theory in the 25µm case. The HR processing improves the system performance to make it nearly equivalent to a 15 to 17µm imaging system.

Our HR processing has also been evaluated onto uniform scene to see the impact of our processing on the temporal noise level but also on the spatial noise. The idea was to check that our method does not degrade such characteristics which are also important in the infrared field. The result is given below (table 1) and shows that at the same time, temporal and spatial noises are improved without any specific additional processing. This aspect will be an interesting development axis for the near future.

Noise measurements gave the following results:

Noise	Procedure	BR	HR
Temporal	Mean standard deviation at each location	8.8	6.6
Spatial	Global standard deviation of an averaged image	89.5	82.9
Global	Quadratic mean	63.6	58.8

Table 1: Temporal and spatial noise measurements

Taking these results into account, one can compute the MRTD given by :

$$\text{MRTD}(f) = \text{NETD} / \text{MTF}(f).$$

By applying this formula to the above data, we can plot the LR and HR MRTDs as seen on figure 4.

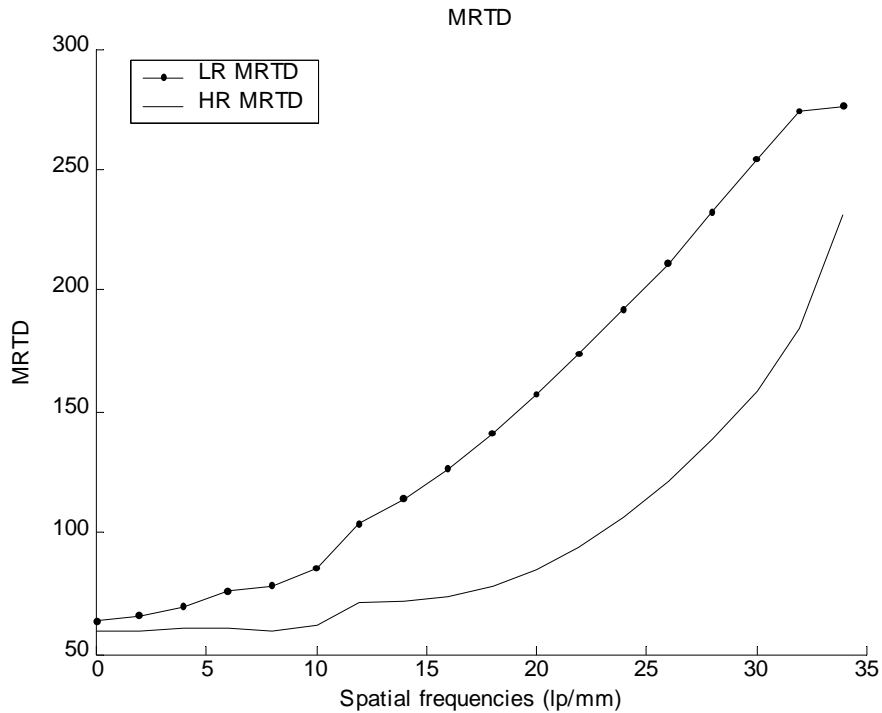


Figure 4: MRTDs for films with (HR MRTD) and without (LR MRTD) HR processing

In order to give a better insight on the above results, we can translate the previous curve at the system level, *i.e.* : in an operational case. So if, as an example, we take a 2.3m x 2.3m $\Delta T=2^{\circ}\text{C}$ with the same optics, detector and electronics, the gain in terms of range will be quite interesting, in case of good weather conditions: see figure 5 below, where the range is shown to be increased by 20% after HR processing.

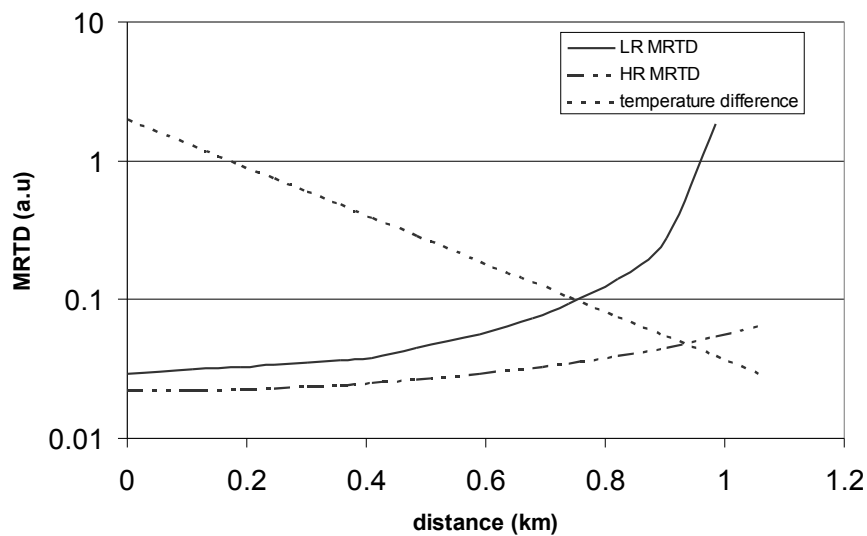


Figure 5: Range comparison with and without HR processing

For visual comparison, we provide an LR image (figure 6) taken at the Nyquist limit as a direct output from the

sensor, and the resulting image (figure 7) obtained after HR processing of a sequence of five such LR images.

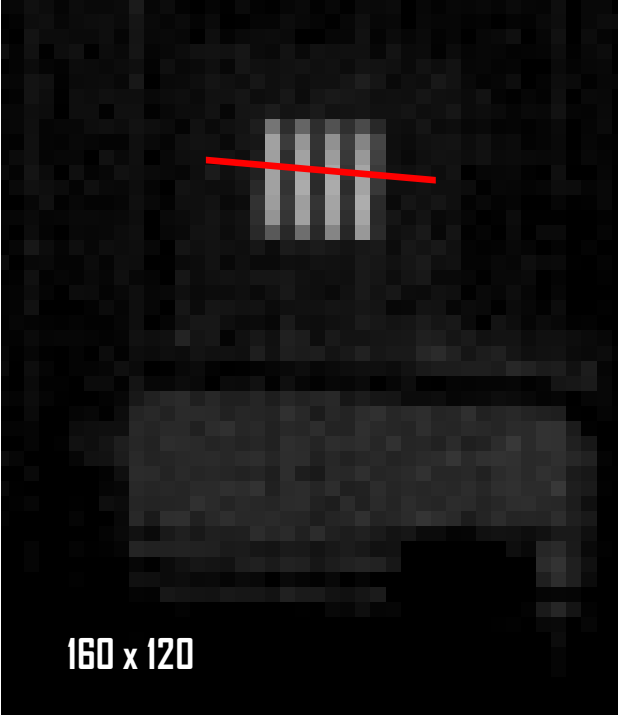


Figure 6: Standard (LR) image output by the sensor. Red line shows the location of an intensity profile.

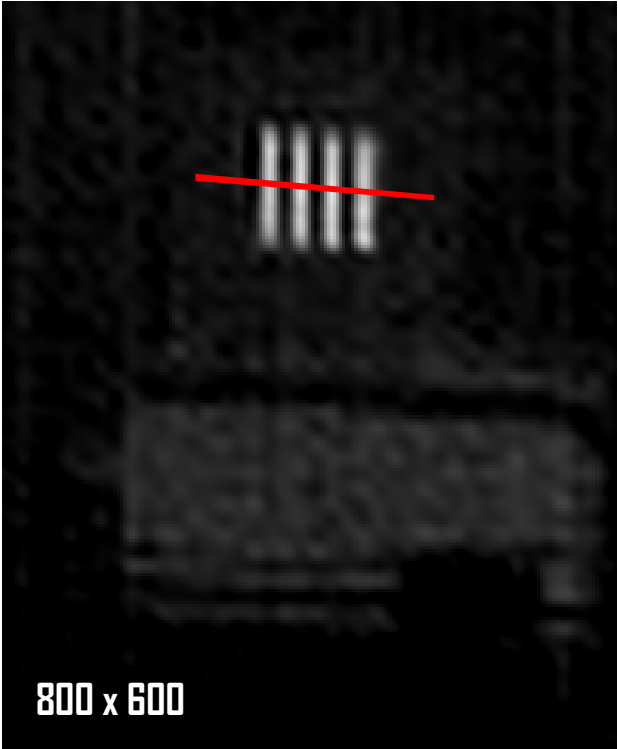


Figure 7: Enhanced (HR) image after HR processing. Red line shows the location of an intensity profile.

2.3 Algorithm benefits

One of the most interesting benefits is to largely improve the resolution without any opto-mechanical devices which kept high the system reliability. Obviously, in the case where the relative movement between the scene and the sensor is fixed, the HR processing has no effect and an opto-mechanical devices will then be necessary but a lot of applications are mobile applications: UAV, automotive, handheld applications... (a small relative displacement is enough). This point can be advantageously used in conjunction with a new figure of merit (FOM) proposed in [7] due to the fact that this new FOM called: dynamic MRTD is well adapted and in any case taking into account relative movement between object and scene.

From the previous results, it is obvious that Lightnics HR enhancement, which takes advantage of the low thermal time constant of microbolometer arrays, enable to improve noticeably such performances as the MTF and MRTD of the global imaging system.

By analyzing the figures, we can explain this improvement by noticing that the HR processing has an impact on both temporal and spatial noise levels, as well as on the contrast of the captured image sequences.

The schematic diagram below is a summarized view to understand the benefit of the HR processing :

Obviously, the resolution can be also improved in only one direction, involving a shorter processing time, for push-broom or process monitoring application for example. This processing is very versatile and will be developed also in the near future for other benefits: spatial noise improvement, stabilization, BPR algorithm...

CONCLUSION

According to these results, cameras equipped with microbolometer arrays and Lightnics HR image processing could perceive both smaller details on a scene and smaller temperature differences. This means that such technology can improve their detectability and range. For example, such system can be used in situations where high magnification zooming is required in order to perceive small and faint objects in the far field. Another interesting application could be in the medical imaging through thermographic diagnosis: our technology could enable a physician to perceive smaller tumors, *i.e.*, start anticipated healing processes.

REFERENCES

- [1] C. D. Kuglin and D. C. Hines, "The phase correlation image alignment method," in Proc. Int. Conf. on Cybernetics and Society, pp. 163–165, IEEE, Sep. 1975.
- [2] Ripley, B.D. (1996) *Pattern Recognition and Neural Networks*, Cambridge: Cambridge University Press, 1996.
- [3] Gareth Williams, *Linear Algebra With Applications*, Jones & Bartlett Publishers, 2005.
- [4] Chellappa, R., Jain, A.K., (Eds.), *Markov Random Fields: Theory and Applications*, Academic Press, 1993.
- [5] A. N. Tikhonov and V. Y. Arsenin, *Solutions of Ill-Posed Problems*, Wiley, New York, 1977.
- [6] J. Coltman, "Specifications of Imaging Properties Response to a Sine Wave Input", J. Opt. Soc. Am., vol. 44, p. 468-, 1954.
- [7] A. Crastes and al., "Uncooled microbolometer trade off or new figure of merit for uncooled imager", Infrared Technology and applications XXXIII, edited by Bjorn F.Andresen, Gabor F. Fulop, Paul P.Norton, Proceedings of SPIE volume 6542, 2007.